Nucleosynthesis simulations in nuclear astrophysics environments

Buttigan, Luka

Undergraduate thesis / Završni rad

2023

Degree Grantor / Ustanova koja je dodijelila akademski / stručni stupanj: **University of Rijeka / Sveučilište u Rijeci**

Permanent link / Trajna poveznica: https://urn.nsk.hr/urn:nbn:hr:194:704143

Rights / Prava: In copyright/Zaštićeno autorskim pravom.

Download date / Datum preuzimanja: **2024-06-27**

UNIVERSITY OF RIJEKA

FACULTY OF PHYSICS

Luka Buttigan

Nucleosynthesis simulations in nuclear astrophysics environments

Bachelor thesis

Rijeka, 28 September 2023

UNIVERSITY OF RIJEKA

FACULTY OF PHYSICS

ASTROPHYSICS AND ELEMENTARY PARTICLE PHYSICS

Bachelor thesis

Nucleosynthesis simulations in nuclear astrophysical environments

Supervisor:

dr. sc. Marina Manganaro

Candidate:

Luka Buttigan

Rijeka, 28 September 2023

Contents

Abstract

This work of thesis is dedicated to the study of nucleosynthesis in astrophysical environments using the NuGrid simulation chain. The process which is most investigated is the r-process in which elements heavier than iron are formed in the interior of stars. The experimental evidence of those processes is not yet possible, but through simulations we investigate the formation of heavy nuclei close to the neutron drip line and search for possible astrophysical data from current experiments can could be used to test the simulations.

Keywords: nuclear astrophysics – simulations – nucleosynthesis – r-process –neutron drip line

Introduction

This work of thesis is focused on the nucleosynthesis of elements, in particular on the synthesis of nuclei heavier than iron. Stellar nucleosynthesis for such heavy nuclei (A> 60) can not be easily probed excprimentally, and even if the processes in which heavier nuclei can be formed in stars are well understood by nuclear physics theory, the direct observation of such processes is nowadays extremely difficult. Nevertheless, a number of astrophysical environments could be studied excprimentally and some violent process as supernova explosion could bring excprimental data to test the current theories in the near future.

In this work we make use of simulations to study the r-process of nucleosynthesis and heavy nuclei close to the neutron drip line. The tools for performing such a study are provided by the NuGrid collaboration and consist in several programs written in FORTRAN and python.

From the simulation of the r-process for different heavy nuclei, we aim to find a possible candidate nucleus that can be studied with existing excprimental data from astrophysics observatories.

1 Nucleosynthesis

The process in which complex nuclei are formed by nuclear reactions, from proton and neutrons is called nucleosynthesis. All the elements present on Earth and in our Universe have been produced in two different stages of nucleosynthesis. The initial nucleosynthesis happened 225s after the Big Bang and its duration was of about 30 minutes. During 30 minutes, light elements up to Lithium (the latter one in very small amounts) have been formed, and the next stage of nucleosynthesis, carried on in the stars, will start only 10^6 years later and it is still going on. At time $t = 225s$ after the Big Bang, the Universe was filled with photons, neutrinos and antineutrinos, electron and nucleons (meaning protons and neutrons). The ratio photons/neutrons/protons was $10^{11} : 13 : 87$ and the Temperature was about $9 \times 10^8 K$. The photons present at this time were those destined to be part of the 2.7 K black body radiation we can observe now as cosmic microwave background. In such conditions, the following nuclear reaction took place beetween protons and neutrons:
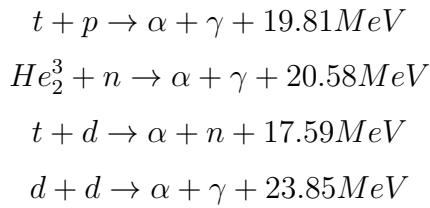
$$n + p \rightarrow d + \gamma + 2.22 \ MeV \tag{1}$$

where d stands for deuteron (H_1^2). This was the first step required in the building of more complex nuclei. Before $t = 225s$, this reaction was also possible, but the temperature of the Universe was too high to permit the deuteron to survive, so deuteron was destroyed for photodisintegration in the reverse reaction of Eq. 1. After $t = 225s$, other nuclear reactions were allowed based on deuteron presence. They were:

$$p + d \rightarrow He_2^3 + \gamma + 5.49 MeV \tag{2}$$

and

$$n + d \rightarrow t + \gamma + 6.26 MeV \tag{3}$$

where t is trithium (H_1^3). He_2^3 and t do not undergo photodisintegration, so they can be involved in the following helium-producing reactions:

$$t + p \rightarrow \alpha + \gamma + 19.81 MeV$$
$$He_2^3 + n \rightarrow \alpha + \gamma + 20.58 MeV$$
$$t + d \rightarrow \alpha + n + 17.59 MeV$$
$$d + d \rightarrow \alpha + \gamma + 23.85 MeV$$

The Big Bang nucleosynthesis stops here: during this phase only the mentioned light nuclei can be formed, with the exception of Lithium in very small amounts because of the following reaction:

$$He_2^4 + t \rightarrow Li_3^7 + \gamma + 2.47 MeV. \tag{4}$$
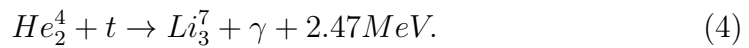
Lithium is readily destroyed in the following reaction:

$$Li_3^7 + p \rightarrow \alpha + \alpha + 17.35 MeV. \tag{5}$$

So only a tiny amount of Lithium could have survived after this first stage of nucleosynthesis.

All the other elements heavier than Lithium has been synthetized in the interior of stars: the stellar nucleosynthesis began 10^6 years later.

1.1 Stellar evolution

A protostar is a cloud of cool interstellar material, composed by hydrogen and helium formed during the Big Bang.

The dynamical equilibrium of the star, also known as hydrostatical equilibrium is essentially a balance between gravity and internal pressure forces. The hydrostatical equilibrium is important because from its equation we derive a crucial theorem for understanding evolution of stars which is known as virial theorem.

$$\frac{\mathrm{d}P}{\mathrm{d}r} = -\frac{GM_r\rho}{r^2} \tag{6}$$

is the equation of hydrostatical equilibrium which multiplied by $4\pi r^3 \mathrm{d}r$ and integrating by parts the resulting equation from the centre to the surface is

$$4\pi \left[r^3 P \right]_{r=0,P=P_\mathrm{c}}^{r=R,P=P_\mathrm{s}\simeq 0} - 3\int_0^R P4\pi r^2 \ \mathrm{d}r = -\int_0^R \overbrace{\frac{GM_r}{r}}^{\frac{GM_r}{r}\frac{\mathrm{d}M_r}{r}} \underbrace{4\pi r^2 \rho \mathrm{d}r}_{\mathrm{d}M_r}. \tag{7}$$

The boundary term vanishes in the center and at the surface while the last term gives gravitational potential energy of the star Ω [1]. If we use the relationship between internal energy and pressure of an ideal gas with an adiabatic exponent γ

$$u = \frac{P}{\gamma - 1} \tag{8}$$

which turns the integral on the left

$$\int_0^R P_r 4\pi r^2 \ \mathrm{d}r = (\gamma - 1)\underbrace{\int_0^R u4\pi r^2 \ \mathrm{d}r}_{U} \tag{9}$$

Combining the equations we obtain the virial theorem:

$$\Omega + 3(\gamma - 1)U = 0 \tag{10}$$

For $\Omega = -2U$ and $\gamma = 5/3$ the total energy $E = \Omega + U$ can be written as

$$E = -U \sim -\frac{3}{2}N\langle kT \rangle \tag{11}$$

From the equation we can intuitively assume that the star losing energy for example, by radiation, E becomes more negative which consequently gives

3

rise in the average temperature [1]. Such change can be explained by the virial theorem that states half the gravitational potential energy resulted from the contraction of a star is converted into thermal energy while the other half is lost from the star.

If we assume an equilibrium state of nuclear fuel burning in the star ϵ and it's perturbation as $\Delta\epsilon$ the perturbation itself will increase the energy production of the core which then causes the expansion of the core. According to the virial theorem, we see the reduction in U and consequently T. Reduction in temperature, then, implies reduction in burning rate which makes nuclear burning stable in non degenerate stars.

If we assume a phase in which there is no nuclear burning, the energy decreases because it's radiated from the surface. If energy decreases so does Ω from the equation $E = \frac{1}{2}\Omega$, which implies star contraction. Calling upon the virial theorem again half of the gravitational potential energy heats the star. When the core reaches high enough temperature some nuclear reactions start to occur. Stars are defined by these cycles of contraction and nuclear burning. In the pre main sequence, the star contracts until the center reaches temperatures for hydrogen burning at around 10^7 K. If the core remains out of hydrogen two things can happen, either it becomes degenerate or has enough temperature in the core for helium burning at temperatures of about 10^8 K. The cycles of contraction and nuclear burning can continue dependent, of course, by the mass of the star, until the core is composed of iron. At that point the core collapses as it can release nuclear energy no further because of iron's highest binding energy which consequently leads to a core collapse supernova.

Such negative feedback between energy and temperature does not work in degenerate matter because, then, the pressure is independent of temperature. Since the burning of nuclear fuel does not cause the core to expand it means the temperature increases as well, which in turn will increase the burning of nuclear fuel. That means in degenerate matter we have a positive feedback that can turn into what is called a thermonuclear runaway observed in certain supernovae.

The mentioned degenerate matter represents an extremely dense form of fermionic matter, characterized by a substantial pressure originating from the Pauli exclusion principle. In the field of astrophysics, this term is employed to describe situations in which gravitational forces reach such intensity within stellar objects that quantum mechanical effects become prominent.

In a fermionic gas primarily governed by thermal effects, a significant portion of electron energy levels remains unoccupied, allowing electrons to freely transition to these states. As the contraction of matter progresses, particle density escalates, leading electrons to progressively occupy lower-

energy states, while additional electrons are compelled to occupy higher-energy states. The resistance to further compression in degenerate gases is substantial because electrons cannot occupy already filled lower-energy levels due to the Pauli exclusion principle. The momentum of fermions within the fermion gas generates a counteracting force known as degeneracy pressure.

Specifically, when referring to electrons, this pressure is termed "electron degeneracy pressure." In scenarios of high density, matter transforms into a degenerate gas when all electrons are separated from their parent atoms. The core of a star, once nuclear fusion reactions cease, undergoes a transformation into a collection of positively charged ions, predominantly helium and carbon nuclei, suspended within a sea of stripped electrons. Pressure increases solely due to the cumulative mass of these particles, intensifying the gravitational force that draws them closer together. Consequently, this phenomenon runs counter to the usual behavior of matter, where an increase in mass results in larger objects. In a degenerate gas, greater mass leads to particles clustering closer together under the influence of gravity, resulting in increased pressure and a smaller overall size. The non relativistic electron degeneracy at 0 K is defined as following [1]:

$$P = K_1 \left(\frac{\rho}{\mu_e m_{\mathrm{H}}} \right)^{5/3} \tag{12}$$

while the relativistic electron degeneracy equation at 0 K looks as following [1]:

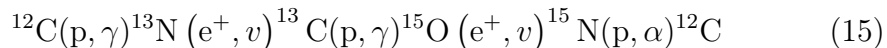$$P = K_2 \left(\frac{\rho}{\mu_e m_{\mathrm{H}}} \right)^{4/3} \tag{13}$$

White dwarfs are a common electron degenerate object but they are bounded by an upper limit from a further collapse called Chandrasekhar limit. The limit is approximately 1.44 solar masses for objects with oxygen and carbon compositions with 2 baryons per electron, such composition is thought to be the usual one for white dwarfs [2].

$$M_{\mathrm{Ch}} = 1.457 \left(\frac{2}{\mu_e} \right)^2 M_\odot \tag{14}$$

Such value of the Chandrasekhar limit of course does not take into account Coulomb corrections nor correct gravitational values derived from general relativity. If we correct for those 2 problems we get a more realistic value of Chandrasekhar limit which is close to 1.38 solar masses. The object's rotation, which counteracts the gravitational force, also changes the limit for any particular object.

Any object above the mass limit is bound to become a neutron star which is formed by the change in Fermi energy which makes it favorable for the electrons to combine with protons to form neutrons in a process called electron capture. The result is a compact neutron matter which gives rise to a neutron degenerate pressure analogous to the electron degenerate pressure present in white dwarfs. Since both the neutron star and the white dwarf are degenerate matter objects it is bound to draw analogies. Another analogy is in regards to the mass limit. What is a Chandrasekhar limit in white dwarfs, it is a Tolman–Oppenheimer–Volkoff limit in neutron stars. Theoretical limit for non-relativistic objects, with inherent ideal neutron degeneracy pressure, is only 0.75 solar masses. However, unlike the Chandrasekhar limit, the more realistic models for defining Tolman–Oppenheimer–Volkoff limit are poorly understood. Above this limit, a neutron star may collapse into a black hole. Now that the possible fates of stellar objects are defined, let's backtrack a bit and look at massive stars and their different stages of evolution from hydrogen burning to silicon burning.

A massive star around $25 M_\odot$ ($T = 3.81 * 10^7$ K, lifetime $= 6.38 * 10^6$ years) has it's hydrogen burning dominated by the CNO cycle.

$$^{12}\text{C}(p, \gamma)^{13}\text{N}\left(e^+, v\right)^{13}\text{C}(p, \gamma)^{15}\text{O}\left(e^+, v\right)^{15}\text{N}(p, \alpha)^{12}\text{C} \tag{15}$$

The end result is 1α particle and two γ, e^+ [3].
Helium burning for the same mass star ($T = 1.96 * 10^8$ K, lifetime $= 6.30 * 10^5$ years) has two principal reactions

$$3\alpha \rightarrow {}^{12}\text{C} \text{ and } {}^{12}\text{C}(\alpha, \gamma)^{16}\text{O} \tag{16}$$
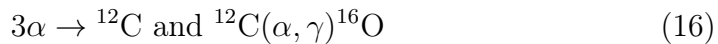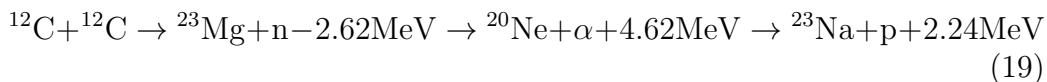
The $^{12}\text{C}(\alpha, \gamma)^{16}\text{O}$ reaction is really important for determining how much carbon is left after helium burning. There are two secondary reactions:
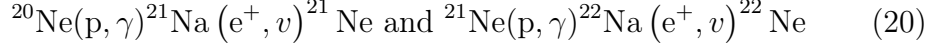
$$^{14}\text{N}(\alpha, \gamma)^{18}\text{F}\left(e^+, v\right)^{18}\text{O} \tag{17}$$

This one happens before helium burning while the following one only happens at high temperatures [4]:

$$^{18}\text{O}(\alpha, \gamma)^{22}\text{Ne} \tag{18}$$
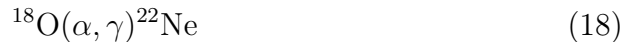
$25 M_\odot$ ($T = 8.41 * 10^8$ K, lifetime $= 9.07 * 10^2$ years) carbon burning in which neutrino losses dominate energy budget. Common reactions are as follows:

$$^{12}\text{C} + {}^{12}\text{C} \rightarrow {}^{23}\text{Mg} + n - 2.62\text{MeV} \rightarrow {}^{20}\text{Ne} + \alpha + 4.62\text{MeV} \rightarrow {}^{23}\text{Na} + p + 2.24\text{MeV} \tag{19}$$

Neutron excess begins to develop:

$$^{20}\text{Ne}(\text{p}, \gamma)^{21}\text{Na}\left(\text{e}^+, v\right)^{21}\text{Ne and } ^{21}\text{Ne}(\text{p}, \gamma)^{22}\text{Na}\left(\text{e}^+, v\right)^{22}\text{Ne} \qquad (20)$$
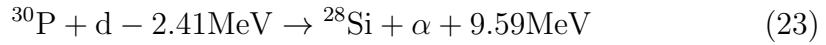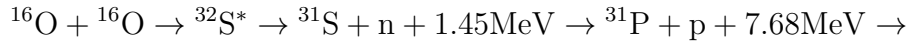
Neon burning for a $25 M_\odot$ star ($T = 1.57 * 10^9$ K, lifetime $= 74$ days) $^{20}\text{Ne}, ^{16}\text{O}, ^{24}\text{Mg}$ are the main components.

$$^{20}\text{Ne}(\gamma, \alpha)^{16}\text{O} \qquad (21)$$

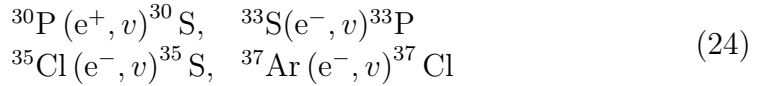$$2\ ^{20}\text{Ne} \rightarrow\ ^{16}\text{O} +\ ^{24}\text{Mg} + 4.59\text{MeV} \qquad (22)$$
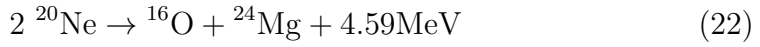
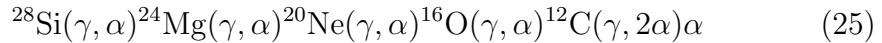As we can see, the abundances of oxygen are increased which implies the next step - oxygen burning.
$25 M_\odot$ star ($T = 2.09 * 10^9$ K, lifetime $= 174$ days), main components $^{28}\text{Si}, ^{16}\text{O}, ^{24}\text{Mg}$. Oxygen burning main reaction is as following [5]:
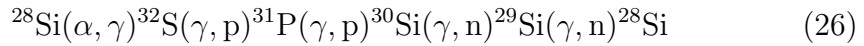
$$^{16}\text{O} +\ ^{16}\text{O} \rightarrow\ ^{32}\text{S}^* \rightarrow\ ^{31}\text{S} + \text{n} + 1.45\text{MeV} \rightarrow\ ^{31}\text{P} + \text{p} + 7.68\text{MeV} \rightarrow$$

$$^{30}\text{P} + \text{d} - 2.41\text{MeV} \rightarrow\ ^{28}\text{Si} + \alpha + 9.59\text{MeV} \qquad (23)$$

Neutron excess reactions:

$$\begin{array}{ll} ^{30}\text{P}\left(\text{e}^+, v\right)^{30}\text{S}, & ^{33}\text{S}(\text{e}^-, v)^{33}\text{P} \\ ^{35}\text{Cl}\left(\text{e}^-, v\right)^{35}\text{S}, & ^{37}\text{Ar}\left(\text{e}^-, v\right)^{37}\text{Cl} \end{array} \qquad (24)$$
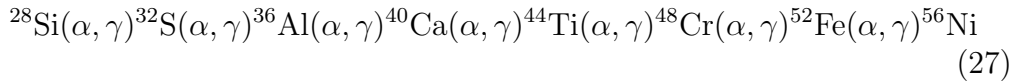
Now all that remains is the last stage, silicon burning. $25 M_\odot$ ($T = 3.65 * 10^9$ K, lifetime $= 1$ day) there is a breakdown in ^{28}Si [6]:

$$^{28}\text{Si}(\gamma, \alpha)^{24}\text{Mg}(\gamma, \alpha)^{20}\text{Ne}(\gamma, \alpha)^{16}\text{O}(\gamma, \alpha)^{12}\text{C}(\gamma, 2\alpha)\alpha \qquad (25)$$

Equilibrium:

$$^{28}\text{Si}(\alpha, \gamma)^{32}\text{S}(\gamma, \text{p})^{31}\text{P}(\gamma, \text{p})^{30}\text{Si}(\gamma, \text{n})^{29}\text{Si}(\gamma, \text{n})^{28}\text{Si} \qquad (26)$$

Now adding iron:

$$^{28}\text{Si}(\alpha, \gamma)^{32}\text{S}(\alpha, \gamma)^{36}\text{Al}(\alpha, \gamma)^{40}\text{Ca}(\alpha, \gamma)^{44}\text{Ti}(\alpha, \gamma)^{48}\text{Cr}(\alpha, \gamma)^{52}\text{Fe}(\alpha, \gamma)^{56}\text{Ni} \qquad (27)$$
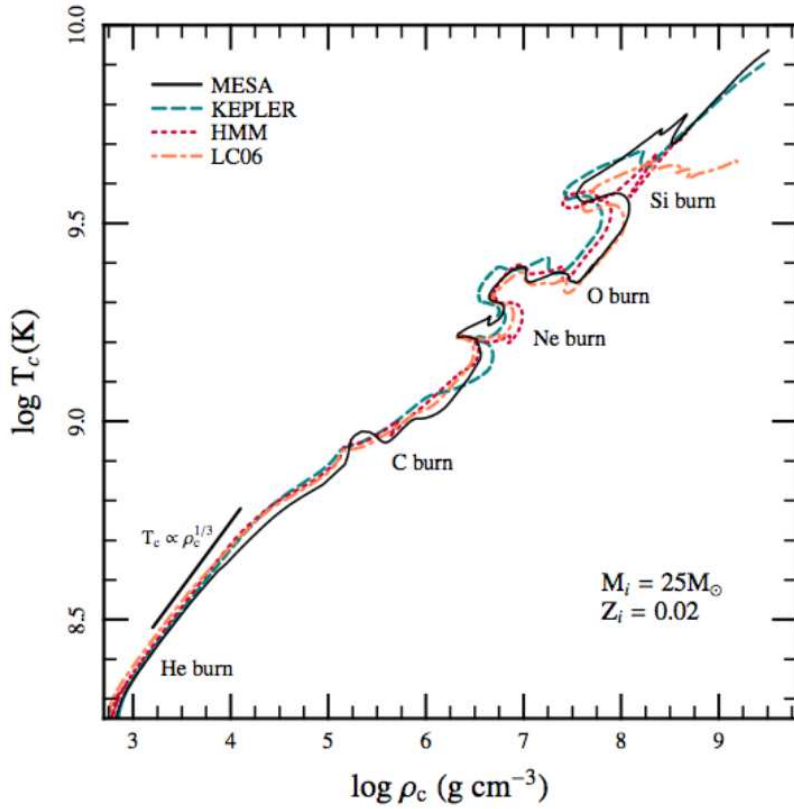
Figure 1: Evolution of central temperature and central density in solar metallicity from different stellar evolution codes [7]

1.2 Stellar nucleosynthesis of heavy elements

1.2.1 s-process

The s-process constitutes significant nucleosynthetic mechanism responsible for synthesis of high mass isotopes and elements. The trajectory of the s-process in the plane of nucleon numbers intersects the closed neutron shells in a region where β-decay doesn't occur. Such observation indicates that s-process occurred within lesser neutron densities compared to r-process. Moreover, s-process transpired over an extended temporal interval. The s-process, characterized as "slow," manifests within massive stars (as the "weak s-process") and stars evolving along the asymptotic giant branch (as the "main s-process") [8, 9, 10]. Weak s-process nucleosynthesis is accountable for generating s-process elements within the lower mass spectrum, spanning from iron-group nuclei up to strontium (Sr) and yttrium (Y) [11]. Abundance peaks indicate that the s-process is a neutron-capture mecha-

8

nism operating within a environment trying to attain balance but not quite achieving it [12]. Primary reactions responsible for driving nucleosynthesis toward the iron group can liberate neutrons that then become captured by pre-existing nuclei, producing s-nuclei.

Elemental abundances that came as a result of the Big Bang were enriched by protons and yield $Y_e = 0.88$. This signifies requirements for conversion of the protons and neutrons into nuclei with the highest binding energy per nucleon for exampe Fe-nuclei, value of Y_e in the universe needs to get lower. Reduction in regards to electron fraction occurs due to weak decays happening in proton-proton chains and Carbon-Nitrogen-Oxygen cycle during the burning of H. Such phenomena cause the electron fraction to decrease from 0.88 to 0.5 in nuclear matter that has undergone the burning of H. The surplus neutrons found in ^{13}C and ^{22}Ne result from the overarching drive to reduce Y_e within stars [13].

1.2.2   r-process

The creation of heavy elements like Thorium (Th) and Uranium (U) hinges significantly on the r-process, which operates under extraordinary conditions characterized by neutron densities ranging from 10^{20} to 10^{28} cm^{-3} and timescales as short as a few seconds. These conditions strongly point to astrophysical events of a explosive nature, such as core collapse Supernovae (SNII), collapsars, and the merging of neutron stars [14, 15, 16, 17], as potential sites where the r-process unfolds.

Within this environment of remarkable neutron densities, seed nuclei rapidly capture a multitude of neutrons within a brief time frame. This process drives the r-process along isotopic chains towards highly neutron-rich species until it attains a state known as "waiting points." Subsequent beta decay to the next higher element sets in motion a new cycle of captures of neutrons, ultimately leading to a new equilibrium. During periods of peak neutron flux, critical parameters come into play, including neutron separation energies that govern the equilibrium between (n, γ) and (γ, n) reactions, as well as the β-decay rates of waiting-point nuclei. These parameters are of utmost importance in determining the duration of the r-process and shaping the distribution of its abundances. Consequently, our primary emphasis is on obtaining precise data concerning the masses and β-half lives of exceedingly neutron-rich nuclei along the r-process pathway [18].

It is crucial to highlight that the conditions required for the r-process are not typically found in simulations of stellar winds. Parametric investigations of neutrino-driven winds have been unable to reproduce the heaviest

element nucleosynthesis observed by [15] due to prerequisites such as electron fractions falling under 0.5, elevated entropy levels with short build-up of timescales, giving a neutron-to-seed ratio over 100.

1.2.3 Weak r-process

Weak r-process is defined by $0.4 < Y_e < 0.5$ and it characterizes slightly neutron rich winds. It is called weak because the neutron to seed ratio, namely $Y_n/Y_{seed} < 0.01$, is much lower compared to the one for the r-process, which has a neutron-to-seed ratio over 100. For said process, to the increase in temperature corresponds a growth of the abundance of seed nuclei. Because the time scales of beta decay are longer than the ones of the wind expansion, the alpha capture is the dominant process which brings to the formation of heavy nuclei. The main products of such a process are Sr, Y and Zr and r-process could then be considered one of the processes bringing to the formation of elements from Sr to Arg in the early Universe. Many nucleosynthesis studies are conducted trying to find wind parameters in the weak r-process context that can provide a match of observed abundances of the lighter heavy nuclei with the predicted ones. Those investigations are not straightforward because of the many uncertainties connected to weak r-process. Recently it has been also proposed through supernova simulations that neutrino wind can contain a considerable amount of protons, which would make important to consider also another process (so called νp).

1.2.4 p-process

Several proton-rich (p-) isotopes of naturally occurring stable nuclei cannot be synthesized through neutron captures along the line of stability [13]. Preferred synthesis for the 35 p-isotopes spanning from ^{74}Se to ^{196}Hg involves a series of neutron, proton, and α-particle photodisintegrations, along with their reverse capture reactions and/or $\beta+$ decays during the late stages of evolution in massive stars [19].

An acknowledged shortcoming of the model is the insufficient production of nuclei within the Mo-Ru region, and a similar underproduction is observed within the region of $151 < A < 167$ [20]. The timescale for proton capture diminishes with a higher availability of protons in the environment. For instance, when $\rho Y_p = 10^3 \, \text{g} \, \text{cm}^{-3}$, the timescale for proton capture on ^{92}Mo is approximately 10 seconds, whereas at $\rho Y_p = 10^6 \, \text{g} \, \text{cm}^{-3}$, it reduces to about 10^{-2} seconds [19, 21]. The conditions conducive to such densities make it improbable to locate the site of the p-process. Furthermore, proton-capture rates escalate with rising temperature due to the heightened relative

kinetic energy of the reactants compared to the Coulomb barrier at lower temperatures [22].

1.2.5 νp-process

The νp-process is observed in explosive scenarios, occurring within the inner ejecta of core-collapse supernovae [23] and potentially in the ejected material from black hole accretion disks in the collapsar model of gamma-ray bursts [24]. This phenomenon manifests when there is an expulsion of proton-rich material driven by intense neutrino fluxes, which can be derived from simulations of supernovae [25, 26].

In regions characterized by winds rich in protons, following the formation of alpha particles (which result from the combination of free neutrons and protons as matter expands and cools), an excess of protons persists. As a consequence of neutrino and antineutrino interactions with neutrons and protons, stemming from ejecta released during core-collapse supernovae, the nucleosynthesis process shifts toward the production of heavier nuclei on the proton-rich side of stability. This occurs due to the differences in mass between neutrons and protons [27]. Alpha particles subsequently merge into heavier nuclei via the triple-α process, with certain nuclei potentially reaching the iron group, depending on expansion and entropy conditions.

In a scenario rich in protons, free protons remain available during the alpha freeze-out phase. As the temperature decreases to approximately 2×10^9 K, the composition of the ejecta becomes predominantly comprised of ^{4}He, protons, and iron group nuclei. These nuclei possess nearly equal numbers of neutrons and protons (N$\approx$Z), primarily including ^{56}Ni and possibly even up to ^{64}Ge, which serve as bottlenecks in the process. These nuclei accumulate during the expansion timescale of the wind due to their relatively long beta decay half-lives ($T_{1/2}$), such as ^{56}Ni with half-life of 6 days and ^{64}Ge with half-life of 64 seconds. [27].

The matter is subjected to a substantial influx of neutrinos and antineutrinos originating from the proto-neutron star. The interaction of antineutrinos with protons generates free neutrons in quantities ranging from 10^{14} to 10^{15} cm^{-3}. These free neutrons are readily captured by heavy, neutron-deficient nuclei like ^{64}Ge, initiating (n,p) reactions with timescales significantly shorter than the beta decay half-life. This process, in turn, facilitates additional proton captures and sustains the nucleosynthesis, allowing for the synthesis of even heavier nuclei. These (n,p) reactions are followed by (p,γ) reactions, enabling the nucleosynthesis process to surmount the bottlenecks posed by ^{56}Ni and ^{64}Ge [27].

1.2.6 i-process

An intermediate form of nucleosynthesis through neutron capture, known as the *i-process*, exists. This mechanism exhibits a neutron flux that surpasses that of the *s*-process but remains below the extreme conditions characteristic of the *r*-process. Within carbon-enhanced metal-poor stars (CEMP-r/s stars), an augmentation of barium (Ba) and europium (Eu) — elements associated with the *s*- and *r*-processes respectively — is observed [28, 29]. Utilizing straightforward single-zone simulations of *i-process* nucleosynthesis, yields are generated that closely match the observed heavy-element abundances spanning from yttrium (Y) to iridium (Ir) in several CEMP-r/s stars, accounting for their inherent observational uncertainties.

In computational models for highly massive asymptotic giant branch (AGB) stars, convective boundary mixing is considered based on a parameterized model [30]. These models suggest that proton-rich material can be mixed into the helium-burning shell convectively, thereby creating conditions conducive to the *i-process*. Notably, the prevalence of *i-process* conditions is more prominent in models characterized by lower metal content, underscoring the heightened significance of the *i-process* during the early stages of the universe.

2 Nuclear Astrophysics

Nuclear Astrophysics is the science connecting Nuclear Physics with the study of our Universe. The origin of the elements in our Universe, as we have described in Chapter 1, is explained by nuclear reactions happened closely after the Big Bang and later in the interior of stars. Even if we have evidence that this is the main way in which elements have been produced, still many parts of the big picture are unclear, especially when it comes to the nucleosynthesis of high mass nuclei. Nuclear Astrophysics aims to understand the origin and distribution of the elements in the universe, from the lightest elements like hydrogen and helium to the heaviest elements like gold and uranium. This requires a detailed understanding of the nuclear reactions that occur in stars and other astrophysical environments, as well as the conditions and mechanisms that drive these reactions. Nuclear astrophysics also seeks to understand the processes of stellar evolution and nucleosynthesis, including the formation and evolution of stars, the production of heavy elements, and the distribution of elements in the universe. This requires a combination of observational data, theoretical models, and computational simulations to capture the complex physical processes involved. Accurate nuclear data and reaction rates are essential for understanding and modeling nuclear reactions in astrophysical environments. However, many of the relevant nuclear reactions involve rare or unstable isotopes that are difficult to produce and measure in the laboratory. Nuclear astrophysics needs to develop new exprimental and theoretical techniques to produce and validate accurate nuclear data.

Neutron stars and other compact objects, such as black holes, present a number of challenges for nuclear astrophysics. These objects involve extreme gravitational and electromagnetic fields, as well as intense radiation and magnetic fields, which can affect the properties and behavior of nuclear matter. Understanding the structure, composition, and behavior of these objects requires a combination of observational and theoretical studies.

Nuclear astrophysics involves a wide range of disciplines, including nuclear physics, astrophysics, astronomy, and computational science. Collaboration and communication among these fields are essential for making progress and addressing the many open questions and challenges in the field. Nuclear astrophysics also needs to engage with other areas of physics and astronomy, such as particle physics and cosmology, to develop a comprehensive understanding of the universe.

3 Neutrino-driven winds

3.1 Core-collapse supernovae

Supernovae, the life cycle's conclusion for massive stars, symbolize an event where stars, at least eight times the sun's mass, lead to either neutron stars or black holes' formation [31, 32]. Generating energy, massive stars burn hydrostatically throughout their existence, and when they produce nuclei heavier than the Fe-peak, this results in energy consumed rather than released, with iron marking the last hydrostatic burning stage, accompanied by the development of concentric layered structure.

When hydrostatic burning halts, fusion reactions no longer exert outward pressure on the core, leading to its contraction. Simultaneously, Si layer burning on top of the iron core's layer increases the core's mass. This can happen because the force from electron degeneracy pressure opposes the gravitational force. However, as core's mass approaches approximately 1.44 mass of the Sun, the electron degeneracy gets overwhelmed by the gravitational force, collapsing the star.

Accelerating core-collapse are two effects: rising concentration of the electrons makes electron capture energy efficient for protons, reducing electron degeneracy pressure, and energy loss occurs due to photodisintegration iron group nuclei into lower mass nuclei, α-particles, protons and neutrons, potentially contributing to pressure.

During core-collapse's initial phase, significant neutrino interactions include elastic scattering on nuclei, (ν_e, ν_e), elastic electron-neutrino scattering, $e^-(\nu_e, \nu_e)e^-$, inverse beta decay, (ν_e, e^-), and inelastic scattering on nuclei, $(\nu_e, \nu_0 e)$ [33]. As core density arrives to $\rho = 10^{12}$ g cm^{-3}, neutrinos become confined due to additional interactions, resulting in longer diffusion times compared to the time for collapse [34]. Collapse persists up to the time when the inner core compresses to densities around $\rho = 10^{14}$ g cm^{-3}, after which it slows down the acceleration, rebounding in response to further increase in density, generating a shock wave. As shock waves traverse outer core, they dissipate energy through photodisintegration that occurs in iron and nickel and neutrino emission.

Exploring core-collapse supernovae mechanisms has been a persistent challenge in supernova theory. Before the concesus was that the shock wave's energy would suffice to halt core-collapse and trigger an explosion of the star's outer shells, the "prompt mechanism." This loss of energy by the shock wave is due to photodisintegration breaking down higher mass nuclei into neutrons, protons and α-particles. Additionally, electron capture occurring to protons further deplete energy, yielding a significant number of electron neutrinos.

Many of them, generated behind the shock, escape the stellar structure, carrying energy, resulting in shock wave stalling at an outer core boundary of approximately 100 to 200 km [35].

Presently, prevailing belief suggests that neutrinos from the core characterized by high temperatures and densities, revive the shock wave, known as the "delayed neutrino-heating mechanism" [36]. The particular fermions move majority of energy, approximately 10^{53} erg, released during the collapse of the iron core and deposit part of the energy prior to reaching the shock [37, 38]. This revitalized shockwave expels the star's outer layers, resulting in a successful explosion. During this process, the outgoing shock wave increases density and temperature of layers with different compositions, leading to the synthesis of nuclei up to $Z = 44$ [39].
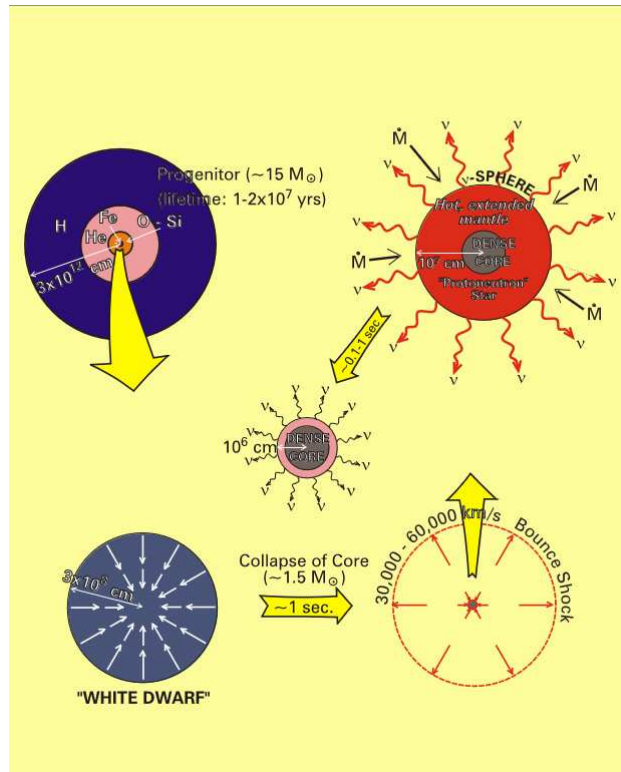

Figure 2: Evolution from the stellar core to the radiating proto-neutron star [40]

3.2   Neutrino-driven winds

Throughout the tumultuous demise of a star with significant mass, it's gravitational potential undergoes a profound change into internal energy, thereby yielding an initial temperature of considerable magnitude for the nascent proto-neutron star (approximately $k_B T \approx 30 - 50$ MeV). Nonetheless, this fervently heated proto-neutron star nuclei can be formedriences a gradual tempering, predominantly instigated by the liberation of neutrinos, functioning as carriers of thermal energy. The proto-neutron star's interior boasts exceedingly elevated densities (roughly $\rho \sim 10^{14}$ g cm^{-3}), initially causing neutrinos to be ensnared within. Subsequently, as they diffuse from the core's depths, they attain mobility when their average displacement distance attains parity with boundary of a neutron star.

Neutrinos emanate of a region known as the neutrinosphere, ensconced within the periphery of a nascent neutron star. Essential is to underscore the fact that the neutrinosphere's location differs for each distinct neutrino flavor and energy, owing to the intricate energy-dependent nature of neutrino-matter interactions [41]. A portion of the neutrinos imparts its energy to the ambient matter through charged-current reactions, typified by processes such as $\nu_e + n \rightarrow p + e^-$ and $\bar{\nu}_e + p \rightarrow n + e^+$.

Aforementioned transference of energy precipitates a substantial fractional expulsion of the outer strata of a nascent neutron star, engendering a phenomenon termed "neutrino-driven wind". This wind materializes subsequent to the cataclysmic supernova eruption and may persist for a duration spanning several seconds or, conceivably, minutes [42].

3.3   Nucleosynthesis in neutrino-driven winds

In vicinity of a newly created neutron star's outer layer, extreme temperatures ($T \geq 10$ GK) induce a state of nuclear statistical equilibrium (NSE). In this phase chemical stability is established between nuclear reactions generating fundamental nuclei (referred to as (Z, A)) and photodissociation reactions disintegrating these atomic cores into nucleons: $(Z, A) \rightleftharpoons (A - Z)n + Zp$. The specific nuclear composition during NSE has been solely dictated by factors such as temperature, density, as well as nucleon concentrations [43].

At elevated temperatures, α particles and nucleons predominate NSE compositions, potentially accompanied by the presence of light clusters (2H, 3H, 3He, 4He). Weak interactions facilitate the conversion of nucleons. While nuclear material dilates and cools, it undergoes transformations. Approximately at $T = 9$ GK, α particles begin to emerge. Subsequently, at even lower temperatures, α particles and nucleons conjoin to construct basic nu-

clei, resulting in a reduction in neutron and proton concentrations.

When NSE disintegrates, occurring approximately at $T \approx 5 - 8$ GK, α particles dominate the nuclear composition, described as α-rich freeze-out. α particles subsequently merge to produce ^{12}C through triple-α reactions, however if there are ample free neutrons, it goes through ^{4}He$(\alpha n, \gamma)^{9}$Be$(\alpha, n)^{12}$C. Formation of Carbon-12 exhibits a pronounced reliance on density, with faster expansions impeding its formation due to inadequate time spent where the three-body reactions occur.

Following this phase, a series of α captures, including (α, n), (α, p), with (n, γ), (n, p), and (p, γ) reactions contingent on neutron concentration within the wind, unfolds. The intricate process has been denoted as α-process [44]. Charged particle reactions come to a halt when temperatures plummet to the point where the Coulomb barrier becomes insurmountable at temperatures of approximately 1 GK. At this juncture, composition is predominantly characterized by α particles, accompanied by fundamental nuclei synthesized in the course of α-process, as well as nucleons. Development of nuclear compositions is intrinsically linked to the abundances of neutrons, protons, and basic nuclei, which are in turn shaped by the wind's specific parameters [45, 46]

4   The NuGrid simulation chain

The nucleosynthesis calculations in the NuGrid simulations were conducted using the post-processing code PPN (*Post-Processing Network*), which was developed by Herwig et al. in 2008 [47] and extended by Pignatari and Herwig in 2012 [48]. PPN is capable of performing both single-zone and multi-zone post-processing simulations. In the context of NuGrid, single-zone simulations refer to calculations along specific thermodynamic trajectories in the star, while multi-zone simulations involve computations in different layers of the star.

PPN receives input data from the stellar structure models generated by MESA simulations. MESA provides detailed information on the physical conditions within the star, including temperature, density, and composition, which are essential for nucleosynthesis calculations. PPN employs a dynamically updated nuclear reaction network, which can encompass more than 5000 nuclear species, ranging from hydrogen (H) to bismuth (Bi), and involves over 50,000 nuclear reactions. [49]

The nuclear reaction network in PPN is self-adjusting and dynamically adapts its size based on the strength of nucleosynthesis fluxes. These fluxes, represented by $\delta Y_i / \delta t_j$, illustrate the variation rates of abundances (Y_i) of nuclear species (X_i) due to reactions (j). Reaction rates utilized in the network are sourced from various references, including the European NACRE compilation [50] and Iliadis et al [51]. for stable nuclides, as well as more recent data from Kunz et al. [52], Fynbo et al.[53], and Imbriani et al. [54] for unstable isotopes. The JINA Reaclib v1.1 library is also employed for specific reactions. [55]

For neutron capture rates by stable nuclides and relevant unstable isotopes, the Kadonis compilation is utilized by NuGrid. However, for the current study, neutron captures are not considered significant. [49]

To perform complete post-processing of the full MESA nova models, NuGrid utilizes the multi-zone parallel frame of PPN (MPPNP). This approach enables the examination of nucleosynthesis in various layers of the star and accounts for the effects of mixing and burning comprehensively. For single thermodynamic trajectories (T, ρ), post-processing is carried out using the single-zone version of PPN (SPPN). Both variants of PPN utilize the same nuclear physics library and package to ensure consistency and accuracy in the nucleosynthesis calculations. [49]

In conclusion, PPN is a robust post-processing code employed in the NuGrid simulations to study nucleosynthesis in stars. Its dynamically updated nuclear reaction networks with a substantial number of species and reactions, coupled with the consideration of various data sources for reaction rates, al-

low for accurate modeling of element production in stars.

5   Results

The nucleosynthesis evolution discussed earlier in the chapter 3 is founded on provided astrophysical circumstances that alter as the progression advances following the explosion and are also contingent upon the progenitor of the supernova [56]. The neutron star's neutrino cooling drives the transformation of the wind and the ensuing fluctuations in wind parameters: expansion time scale, entropy, and electron fraction [57, 45]. An exhaustive and internally consistent investigation into the significance of particular reactions on the compositions would necessitate an assessment of all conceivable astrophysical conditions, a task exceeding the confines of the current study. In this work, I put forth an initial approach where I investigate diverse nucleosynthesis progressions (i.e., pathways across the nuclear chart) by modifying the electron fraction. By doing so, one can ascertain the circumstances under which a reaction holds importance. I opted to manipulate Y_e since it is the variable exhibiting the greatest uncertainty arising from hydrodynamical simulations. The way electron fraction was controlled is by changing the initial abundance of neutrons.

The runs were made keeping the entropy ($S \approx 175\,k_B/\text{nuc}$) and expansion time scale ($\tau = 5\,\text{ms}$). There are a few peaks in the elemental abundance (figure 3), most notably around Be, then near the area of Sr, Y, Zr production and later the highest elemental abundance is exhibited in In. As it's evident that the majority of the graph follows a simple pattern, lower the electron fraction, higher the elemental abundance. This has a simple explanation, as said earlier, the electron fraction depends on the amount of initial abundance of neutrons set before the run. Higher the amount of neutrons, lower the Y_e. Essentially every run with lower Y_e has more nucleonic matter compared to the higher counterpart which explains the general trend of discrepancy in elemental abundances between the two.

The two lines parallel to the ordinate axis in figure 4 indicate the region between He and B where few interesting results emerge, firstly He abundances deviate from a general pattern of "higher elemental abundance due to lower Y_e", the elemental abundances seem to converge. Which is completely logical since in the runs the initial abundance of He can be tweaked alongside the neutron abundance, however in these 10 runs the He initial abundances were not tweaked so it's expected to have the elemental abundances converge at this particular element. Li however exhibits a peculiar pattern only shared with B and not with any other element in the elemental
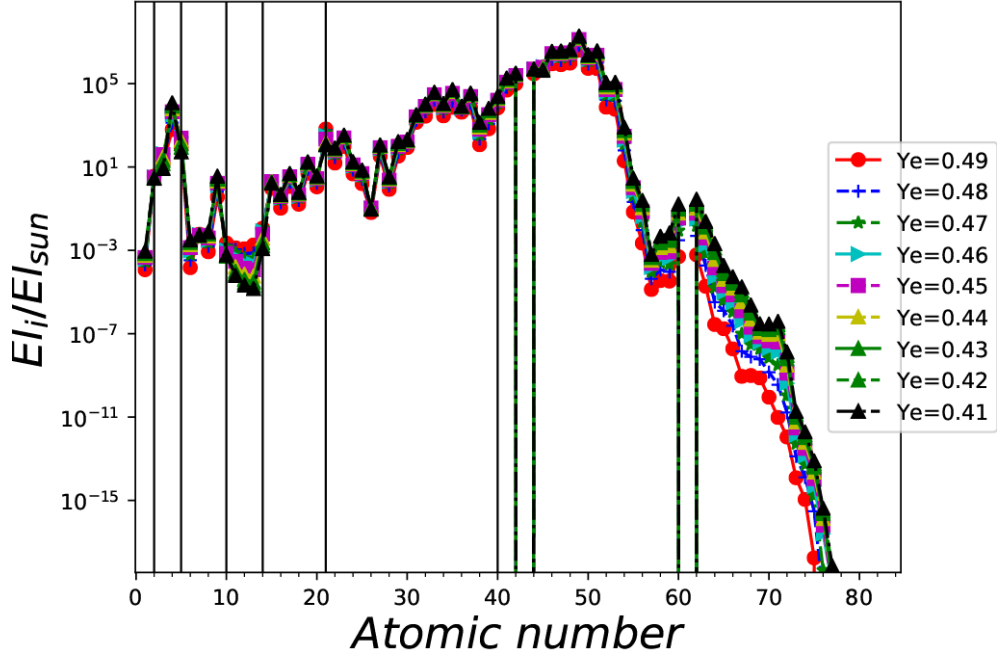
Figure 3: Elemental abundance graph of 10 runs with varied Y_e

abundance graph where both extremes of electron fraction have the lowest elemental abundances. Besides by far the most common pattern mentioned earlier, the other pattern that is not common but in frequency is second only to the most dominant pattern, is the "reversed pattern" which is essentially the higher the electron fraction, the higher the elemental abundance. This pattern in visible in a few places on the elemental abundance graph like figure 5 and figure 6
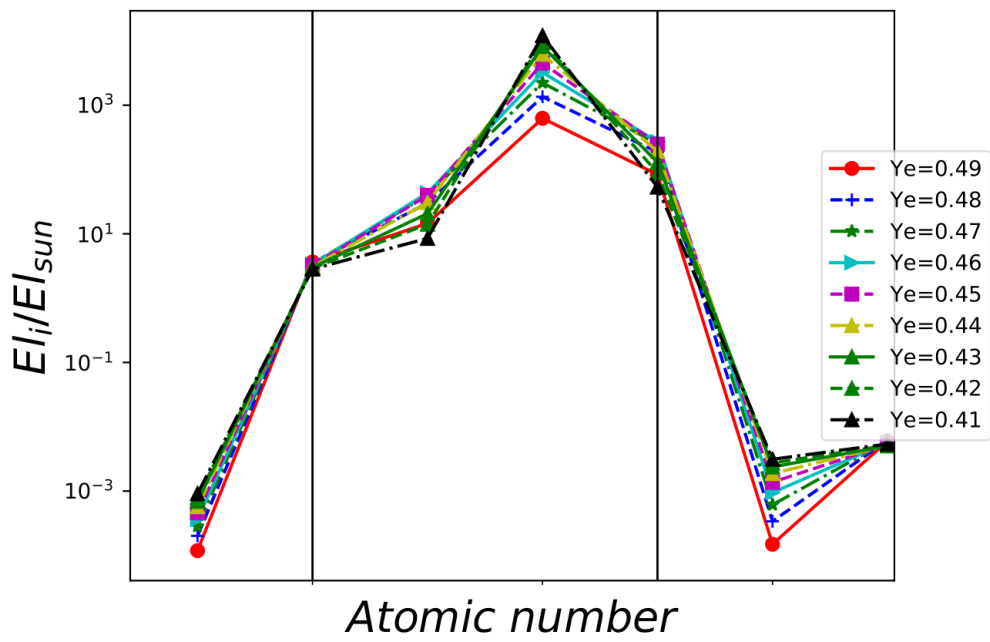
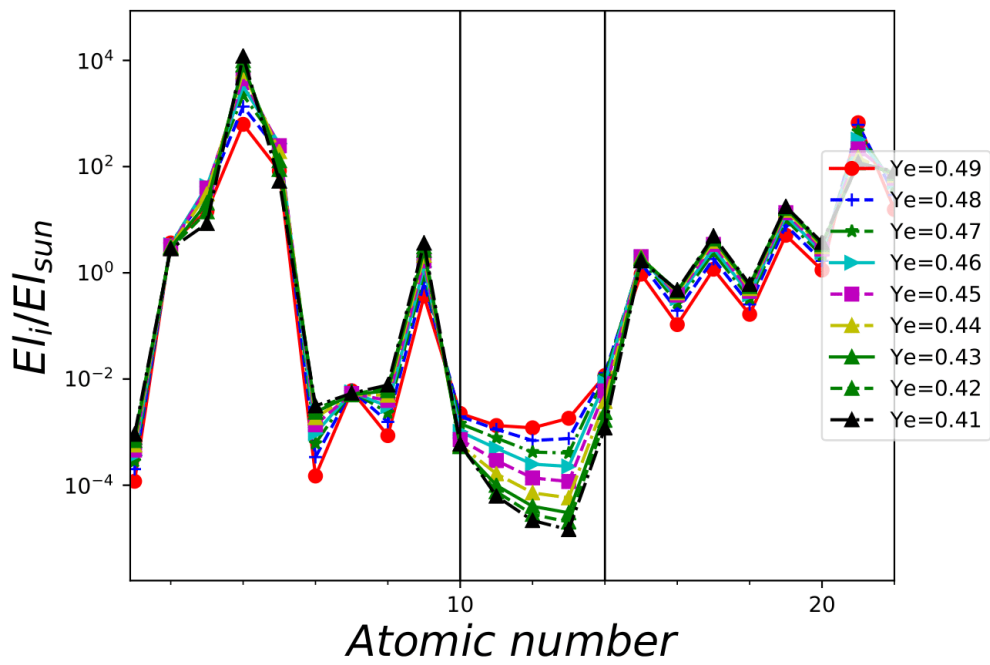Figure 4: Zoomed in part of the figure 3 between H and C

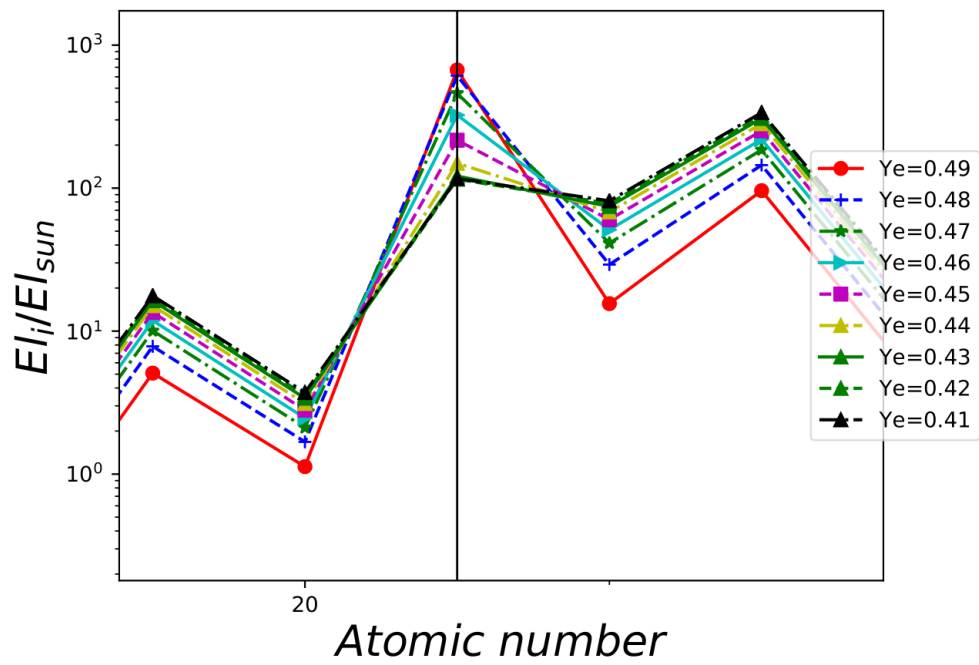Figure 5: "Reversed pattern" elemental abundances between Ne and Si

Figure 6: "Reversed pattern" elemental abundance for Sc

6 Conclusions

Core-collapse supernovae, awe-inspiring events that mark the culmination of massive star lifecycles, are cosmic spectacles of immense energy release. Stars with at least 8 times the mass of our sun exhaust their nuclear fuel, leading to a collapse under gravity's relentless pull. This collapse births either neutron stars or black holes and initiates a cascade of intricate processes that sculpt the cosmos.

At the heart of these cataclysmic events lies neutrino-driven winds, a phenomenon fueled by the intense interplay between the collapsing core and neutrinos – elusive, nearly massless particles that interact weakly with matter. As the core collapses, its gravitational energy transforms into internal energy, resulting in a hot proto-neutron star. The emission of neutrinos from this star carries away energy, and at densities around $10^{14} g/cm^3$, neutrinos become trapped, diffusing through the star. Eventually, they escape from the neutrinosphere, releasing energy into the surrounding matter and initiating a neutrino-driven wind.

This wind is a crucible for nucleosynthesis, the process by which elements are forged through nuclear reactions. Within the high temperatures of the proto-neutron star's outer layers, nuclear statistical equilibrium (NSE) reigns, a state where a delicate equilibrium is maintained between nuclear reactions forming seed nuclei and photodissociation reactions breaking them down into neutrons and protons. As the proto-neutron star expands and cools, the composition evolves, leading to the synthesis of alpha particles, nuclei, and clusters.

As the temperature drops further, the alpha-rich freeze-out sets in, where alpha particles combine to form heavier elements like carbon. Subsequent reactions, such as alpha captures and beta decays, contribute to the formation of even heavier elements. These dynamic processes give rise to distinct patterns of abundance for elements, offering a glimpse into the cosmic history of nucleosynthesis.

To unravel the intricacies of nucleosynthesis within these cataclysmic events, scientists employ sophisticated computational tools like the NuGrid simulation chain. This framework integrates detailed stellar structure models with dynamically updated nuclear reaction networks, allowing for accurate modeling of element production. By simulating post-processing of these models, researchers can study how varying conditions lead to different elemental abundances, providing insights into the origins of the elements that constitute our universe.

In unveiling the enigmatic mechanisms that govern core-collapse supernovae and nucleosynthesis, we deepen our comprehension of the universe's

inner workings. Each revelation brings us closer to understanding the cosmic processes that have shaped our existence, and in this cosmic journey of exploration, we continue to uncover the remarkable story of how the elements themselves were born from the fiery hearts of collapsing stars.

References

[1] Philipp Podsiadlowski. The structure and evolution of stars. URL `http://www-astro.physics.ox.ac.uk/~podsi/stars_summary.pdf`.

[2] E. Öpik. BOOKS (with comments): "Contemporary Astronomy", by J. M. Pasachoff a Review with Particular Reference to Martian Polar Caps. *Irish Astronomical Journal*, 13:145, September 1977.

[3] Kenneth S. Krane. *Introductory Nuclear Physics*. 1987.

[4] F. Kaeppeler, M. Wiescher, U. Giesen, J. Goerres, I. Baraffe, M. El Eid, C. M. Raiteri, M. Busso, R. Gallino, M. Limongi, and A. Chieffi. Reaction Rates for 18O(alpha , gamma) 22Ne, 22Ne(alpha , gamma) 26Mg, and 22Ne(alpha , n) 25Mg in Stellar Helium Burning and s-Process Nucleosynthesis in Massive Stars. , 437:396, December 1994. doi: 10.1086/175004.

[5] P. Brimblecombe. The Global Sulfur Cycle. *Treatise on Geochemistry*, 8:682, December 2003. doi: 10.1016/B0-08-043751-6/08134-2.

[6] Stanford Earl Woosley. Advanced stages of stellar evolution – ii silicon burning and nse. URL `https://www.ucolick.org/~woosley/ay220-19/lectures/lecture12.pdf`.

[7] Bill Paxton, Lars Bildsten, Aaron Dotter, Falk Herwig, Pierre Lesaffre, and Frank Timmes. Modules for Experiments in Stellar Astrophysics (MESA). , 192(1):3, January 2011. doi: 10.1088/0067-0049/192/1/3.

[8] Amanda I. Karakas, D. A. García-Hernández, and Maria Lugaro. Heavy Element Nucleosynthesis in the Brightest Galactic Asymptotic Giant Branch Stars. , 751(1):8, May 2012. doi: 10.1088/0004-637X/751/1/8.

[9] M. Busso, R. Gallino, and G. J. Wasserburg. Nucleosynthesis in Asymptotic Giant Branch Stars: Relevance for Galactic Enrichment and Solar System Formation. , 37:239–309, January 1999. doi: 10.1146/annurev.astro.37.1.239.

[10] S. Bisterzo, R. Gallino, O. Straniero, S. Cristallo, and F. Käppeler. The s-process in low-metallicity stars - II. Interpretation of high-resolution spectroscopic observations with asymptotic giant branch models. , 418 (1):284–319, November 2011. doi: 10.1111/j.1365-2966.2011.19484.x.

[11] F. Käppeler, R. Gallino, S. Bisterzo, and Wako Aoki. The s process: Nuclear physics, stellar models, and observations. *Reviews of Modern Physics*, 83(1):157–194, January 2011. doi: 10.1103/RevModPhys.83. 157.

[12] Terry P. Walker, Gary Steigman, David N. Schramm, Keith A. Olive, and Ho-Shik Kang. Primordial Nucleosynthesis Redux. , 376:51, July 1991. doi: 10.1086/170255.

[13] Bradley S. Meyer. The r-, s-, and p-Processes in Nucleosynthesis. , 32: 153–190, January 1994. doi: 10.1146/annurev.aa.32.090194.001101.

[14] E. Margaret Burbidge, G. R. Burbidge, William A. Fowler, and F. Hoyle. Synthesis of the Elements in Stars. *Reviews of Modern Physics*, 29(4): 547–650, January 1957. doi: 10.1103/RevModPhys.29.547.

[15] S. E. Woosley, J. R. Wilson, G. J. Mathews, R. D. Hoffman, and B. S. Meyer. The r-Process and Neutrino-heated Supernova Ejecta. , 433:229, September 1994. doi: 10.1086/174638.

[16] Shin-ichirou Fujimoto, Masa-aki Hashimoto, Kei Kotake, and Shoichi Yamada. Heavy-Element Nucleosynthesis in a Collapsar. , 656(1):382– 392, February 2007. doi: 10.1086/509908.

[17] Yutaka Komiya and Toshikazu Shigeyama. Contribution of Neutron Star Mergers to the r-Process Chemical Evolution in the Hierarchical Galaxy Formation. , 830(2):76, October 2016. doi: 10.3847/0004-637X/830/2/ 76.

[18] Debra L. Burris, Catherine A. Pilachowski, Taft E. Armandroff, Christopher Sneden, John J. Cowan, and Henry Roe. Neutron-Capture Elements in the Early Galaxy: Insights from a Large Sample of Metal-poor Giants. , 544(1):302–319, November 2000. doi: 10.1086/317172.

[19] M. Rayet, M. Arnould, and N. Prantzos. The p-process revisited. , 227 (1):271–281, January 1990.

[20] Jacob Lund Fisker, Robert D. Hoffman, and Jason Pruet. On the Origin of the Lightest Molybdenum Isotopes. , 690(2):L135–L139, January 2009. doi: 10.1088/0004-637X/690/2/L135.

[21] M. Rayet, M. Arnould, M. Hashimoto, N. Prantzos, and K. Nomoto. The p-process in Type II supernovae. , 298:517, June 1995.

[22] Shinya Wanajo and Yuhri Ishimaru. r-process calculations and Galactic chemical evolution. , 777:676–699, October 2006. doi: 10.1016/j. nuclphysa.2005.10.012.

[23] R. Buras, H. Th. Janka, M. Rampp, and K. Kifonidis. Two-dimensional hydrodynamic core-collapse supernova simulations with spectral neutrino transport. II. Models for different progenitor stars. , 457(1):281–308, October 2006. doi: 10.1051/0004-6361:20054654.

[24] R. Surman, G. C. McLaughlin, and W. R. Hix. Nucleosynthesis in the Outflow from Gamma-Ray Burst Accretion Disks. , 643(2):1057–1064, June 2006. doi: 10.1086/501116.

[25] M. Liebendörfer, A. Mezzacappa, O.E.B. Messer, G. Martinez-Pinedo, W.R. Hix, and F.-K. Thielemann. The neutrino signal in stellar core collapse and postbounce evolution. *Nuclear Physics A*, 719:C144–C152, 2003. ISSN 0375-9474. doi: https://doi.org/10.1016/S0375-9474(03) 00984-9. URL `https://www.sciencedirect.com/science/article/pii/S0375947403009849`.

[26] J. Pruet, S. E. Woosley, R. Buras, H.-T. Janka, and R. D. Hoffman. Nucleosynthesis in the hot convective bubble in core-collapse supernovae. *The Astrophysical Journal*, 623(1):325, apr 2005. doi: 10.1086/428281. URL `https://dx.doi.org/10.1086/428281`.

[27] F. K. Thielemann, I. Dillmann, K. Farouqi, T. Fischer, C. Fröhlich, A. Kelic-Heil, I. Korneev, K. L. Kratz, K. Langanke, M. Liebendörfer, I. V. Panov, G. Martinez-Pinedo, and T. Rauscher. The r-, p-, and νp-Process. In *Journal of Physics Conference Series*, volume 202 of *Journal of Physics Conference Series*, page 012006, January 2010. doi: 10.1088/1742-6596/202/1/012006.

[28] P. S. Barklem, N. Christlieb, T. C. Beers, V. Hill, J. Holmberg, B. Marsteller, S. Rossi, F. J. Zickgraf, and M. S. Bessell. The Hamburg/ESO R-process Enhanced Star survey (HERES): Abundances. In Vanessa Hill, Patrick Francois, and Francesca Primas, editors, *From Lithium to Uranium: Elemental Tracers of Early Cosmic Evolution*, volume 228, pages 201–206, January 2005. doi: 10.1017/S1743921305005557.

[29] T. Masseron, J. A. Johnson, B. Plez, S. van Eck, F. Primas, S. Goriely, and A. Jorissen. A holistic approach to carbon-enhanced metal-poor stars. , 509:A93, January 2010. doi: 10.1051/0004-6361/200911744.

[30] L. Dardelet, C. Ritter, P. Prado, E. Heringer, C. Higgs, S. Sandalski, S. Jones, P. Denissenkov, K. Venn, M. Bertolli, M. Pignatari, P. Woodward, and F. Herwig. The i-process and CEMP-r/s stars. *arXiv e-prints*, art. arXiv:1505.05500, May 2015. doi: 10.48550/arXiv.1505.05500.

[31] Marcella Ugliano, Hans-Thomas Janka, Andreas Marek, and Almudena Arcones. Progenitor-explosion Connection and Remnant Birth Masses for Neutrino-driven Supernovae of Iron-core Progenitors. , 757(1):69, September 2012. doi: 10.1088/0004-637X/757/1/69.

[32] Thomas Ertl, Marcella Ugliano, Hans-Thomas Janka, Andreas Marek, and Almudena Arcones. Erratum: "Progenitor-explosion Connection and Remnant Birth Masses for Neutrino-driven Supernovae of Iron-core Progenitors" <A href="/abs/2012ApJ...757...69U">(2012, ApJ, 757, 69)</A>. , 821(1):69, April 2016. doi: 10.3847/0004-637X/821/1/69.

[33] Stephen W. Bruenn and W. C. Haxton. Neutrino-Nucleus Interactions in Core-Collapse Supernovae. , 376:678, August 1991. doi: 10.1086/170316.

[34] H. A. Bethe. Supernova mechanisms. *Rev. Mod. Phys.*, 62:801–866, Oct 1990. doi: 10.1103/RevModPhys.62.801. URL https://link.aps.org/doi/10.1103/RevModPhys.62.801.

[35] Julia Barbara Erika Bliss. *Nucleosynthesis of lighter heavy elements in neutrino-driven winds*. PhD thesis, Technische Universität, Darmstadt, 2018.

[36] James R. Wilson and Ronald W. Mayle. Report on the progress of supernova research by the livermore group. *Physics Reports*, 227(1):97–111, 1993. ISSN 0370-1573. doi: https://doi.org/10.1016/0370-1573(93)90059-M. URL https://www.sciencedirect.com/science/article/pii/037015739390059M.

[37] A Burrows. Neutrinos from supernova explosions. *Annual Review of Nuclear and Particle Science*, 40(1):181–212, 1990. doi: 10.1146/annurev.ns.40.120190.001145. URL https://doi.org/10.1146/annurev.ns.40.120190.001145.

[38] H. A. Bethe and J. R. Wilson. Revival of a stalled supernova shock by neutrino heating. , 295:14–23, August 1985. doi: 10.1086/163343.

[39] Shinya Wanajo, Bernhard Müller, Hans-Thomas Janka, and Alexander Heger. Nucleosynthesis in the Innermost Ejecta of Neutrino-driven Supernova Explosions in Two Dimensions. , 852(1):40, January 2018. doi: 10.3847/1538-4357/aa9d97.

[40] Adam Burrows. Colloquium: Perspectives on core-collapse supernova theory. *Rev. Mod. Phys.*, 85:245–261, Feb 2013. doi: 10.1103/RevModPhys.85.245. URL https://link.aps.org/doi/10.1103/RevModPhys.85.245.

[41] Shoichi Yamada, Hans-Thomas Janka, and Hideyuki Suzuki. Neutrino transport in type II supernovae: Boltzmann solver vs. Monte Carlo method. , 344:533–550, April 1999. doi: 10.48550/arXiv.astro-ph/9809009.

[42] Robert C. Duncan, Stuart L. Shapiro, and Ira Wasserman. Neutrino-driven Winds from Young, Hot Neutron Stars. , 309:141, October 1986. doi: 10.1086/164587.

[43] J. Bliss, A. Arcones, F. Montes, and J. Pereira. Impact of (α, n) reactions on weak r-process in neutrino-driven winds. *Journal of Physics G Nuclear Physics*, 44(5):054003, May 2017. doi: 10.1088/1361-6471/aa63bd.

[44] S. E. Woosley and Robert D. Hoffman. The alpha -Process and the r-Process. , 395:202, August 1992. doi: 10.1086/171644.

[45] Y. Z. Qian and S. E. Woosley. Nucleosynthesis in Neutrino-driven Winds. I. The Physical Conditions. , 471:331, November 1996. doi: 10.1086/177973.

[46] Todd A. Thompson, Adam Burrows, and Bradley S. Meyer. The physics of proto-neutron star winds: Implications for r-process nucleosynthesis. *The Astrophysical Journal*, 562(2):887, dec 2001. doi: 10.1086/323861. URL https://dx.doi.org/10.1086/323861.

[47] F. Herwig, S. Diehl, C. L. Fryer, R. Hirschi, A. Hungerford, G. Magkotsios, M. Pignatari, G. Rockefeller, F. X. Timmes, P. Young, and M. E. Bennet. Nucleosynthesis simulations for a wide range of nuclear production sites from NuGrid. In *Nuclei in the Cosmos (NIC X)*, page E23, January 2008. doi: 10.22323/1.053.0023.

[48] Marco Pignatari and Falk Herwig. The nugrid research platform: A comprehensive simulation approach for nuclear astrophysics. *Nuclear*

Physics News, 22(4):18–23, 2012. doi: 10.1080/10619127.2012.710142. URL https://doi.org/10.1080/10619127.2012.710142.

[49] P. A. Denissenkov, J. W. Truran, M. Pignatari, R. Trappitsch, C. Ritter, F. Herwig, U. Battino, K. Setoodehnia, and B. Paxton. MESA and Nu-Grid simulations of classical novae: CO and ONe nova nucleosynthesis. , 442(3):2058–2074, August 2014. doi: 10.1093/mnras/stu1000.

[50] C. Angulo, M. Arnould, M. Rayet, P. Descouvemont, D. Baye, C. Leclercq-Willain, A. Coc, S. Barhoumi, P. Aguer, C. Rolfs, R. Kunz, J. W. Hammer, A. Mayer, T. Paradellis, S. Kossionides, C. Chronidou, K. Spyrou, S. degl'Innocenti, G. Fiorentini, B. Ricci, S. Zavatarelli, C. Providencia, H. Wolters, J. Soares, C. Grama, J. Rahighi, A. Shotter, and M. Lamehi Rachti. A compilation of charged-particle induced thermonuclear reaction rates. , 656(1):3–183, August 1999. doi: 10.1016/S0375-9474(99)00030-5.

[51] Christian Iliadis, John M. D'Auria, Sumner Starrfield, William J. Thompson, and Michael Wiescher. Proton-induced thermonuclear reaction rates for a = 20–40 nuclei. *The Astrophysical Journal Supplement Series*, 134(1):151, may 2001. doi: 10.1086/320364. URL https://dx.doi.org/10.1086/320364.

[52] R. Kunz, M. Fey, M. Jaeger, A. Mayer, J. W. Hammer, G. Staudt, S. Harissopulos, and T. Paradellis. Astrophysical Reaction Rate of ^{12}C$(\alpha, \gamma)^{16}$O. , 567(1):643–650, March 2002. doi: 10.1086/338384.

[53] H O U Fynbo, Christian Aaen Diget, U C Bergmann, M J G Borge, J Cederkall, P Dendooven, L M Fraile, S Franchoo, V N Fedosseev, B R Fulton, W X Huang, J Huikari, H B Jeppesen, A S Jokinen, P Jones, B R Jonson, U Koster, K Langanke, M Meister, T Nilsson, G Nyman, Y Prezado, K Rilsager, S Rinta-Antila, O Tengblad, M Turrion, Y B Wang, L Weissman, K Wilhelmsen, J Aysto, and ISOLDE Collaboration. Revised rates for the stellar triple-alpha process from measurement of c-12 nuclear resonances. *Nature*, 433(7022):136–139, January 2005. ISSN 0028-0836. doi: 10.1038/nature03219.

[54] Imbriani, G., Costantini, H., Formicola, A., Vomiero, A., Angulo, C., Bemmerer, D., Bonetti, R., Broggini, C., Confortola, F., Corvisiero, P., Cruz, J., Descouvemont, P., Fülöp, Z., Gervino, G., Guglielmetti, A., Gustavino, C., Gyürky, Gy., Jesus, A. P., Junker, M., Klug, J.

N., Lemut, A., Menegazzo, R., Prati, P., Roca, V., Rolfs, C., Romano, M., Rossi-Alvarez, C., Schümann, F., Schürmann, D., Somorjai, E., Straniero, O., Strieder, F., Terrasi, F., and Trautvetter, H. P. S-factor of 14n(p, at astrophysical energies. *Eur. Phys. J. A*, 25 (3):455–466, 2005. doi: 10.1140/epja/i2005-10138-7. URL `https://doi.org/10.1140/epja/i2005-10138-7`.

[55] Richard H. Cyburt, A. Matthew Amthor, Ryan Ferguson, Zach Meisel, Karl Smith, Scott Warren, Alexander Heger, R. D. Hoffman, Thomas Rauscher, Alexander Sakharuk, Hendrik Schatz, F. K. Thielemann, and Michael Wiescher. The JINA REACLIB Database: Its Recent Updates and Impact on Type-I X-ray Bursts. , 189(1):240–252, July 2010. doi: 10.1088/0067-0049/189/1/240.

[56] A. Arcones and H. Th. Janka. Nucleosynthesis-relevant conditions in neutrino-driven supernova outflows. II. The reverse shock in two-dimensional simulations. , 526:A160, February 2011. doi: 10.1051/0004-6361/201015530.

[57] R. D. Hoffman, S. E. Woosley, and Y. Z. Qian. Nucleosynthesis in Neutrino-driven Winds. II. Implications for Heavy Element Synthesis. , 482(2):951–962, June 1997. doi: 10.1086/304181.